DRAL
Daresbury Laboratory
Rutherford Appleton Laboratory

RAL Report
RAL-94-078

Neutron Compton Scattering

HEP

J Mayers

July 1994

Rutherford Appleton Laboratory Chilton DIDCOT Oxfordshire OX11 0QX

Neutron Compton Scattering

J. Mayers and A.C. Evans
(Rutherford Appleton Laboratory)

1. Introduction

The possibility of measuring atomic momentum distributions in condensed matter sytems by neutron scattering was first suggested by Hohenberg and Platzmann [1] nearly 30 years ago. The method is analagous to the measurement of electron momentum distributions by Compton scattering [2] and measurement of nucleon momenta by Deep Inelastic Scattering [3] and is known as Neutron Compton Scattering (NCS) or Deep Inelastic Neutron Scattering (DINS). The principle is the same in each case; the momentum distribution of target particles (electrons, components of nuclei or atoms respectively) is measured by inelastic scattering of high energy incident particles (photons, electrons or neutrons). The Impulse Approximation (IA), which is exact in the limit of infinite momentum transfer, [4,5,6] is used in the interpretation of NCS measurements and large incident energies are required to keep deviations from the IA small. NCS measurements on most systems have only become feasible with the development of the new generation of pulsed neutron sources such as ISIS at the Rutherford Appleton Laboratory, U.K., IPNS at Argonne, USA, LANSCE at Los Alamos, USA and the KEK source in Japan. . For accurate NCS measurements energy transfers ~100 times greater than the mean atomic kinetic are required and only pulsed neutron sources can supply a sufficiently high intensity of neutrons at the energies required to satisfy this condition. A futher advantage of accelerator sources for these measurements is that the short time pulse (~ 1-2 μsec) allows the use time of flight measurement techniques to measure energy transfers in the eV region with good resolution.

Many early NCS measurements were performed on helium at relatively low energy and momentum transfers, ($\omega < 300$ meV and $q < 15$ Å^{-1}) on reactor sources. These studies were motivated primarily by the possibility of directly observing the Bose condensate fraction in superfluid ^{4}He [7,8,9,10,11]. However despite the low kinetic energy of atoms in superfluid helium, the interpretation of NCS measurements on ^{4}He at such low momentum transfers is complicated by deviations from the IA known generically as Final

State Effects (FSE) [12]. More recently NCS measurements with $15<q<40$ Å^{-1} and incident energies up to 2 eV have been made on condensed phases of helium[13] and neon[14] at IPNS. There have been a few pioneering studies on various systems at eV energy transfers [15,16,17].

The electron volt spectrometer (eVS) at ISIS [18,19] has been dedicated to the development of the NCS technique during the last five years and now has a full user program which is demonstrating the potential of this new neutron scattering technique for providing unique and detailed information about the atomic wavefunction and atomic kinetic energies in condensed matter. NCS has applications to all areas of neutron science e.g. quantum fluids, molecular science, liquid metals, amorphous and non crystalline materials, hydrogen bonds, atomic and molecular hydrogen in materials and many other areas. In this article we will discuss the type of information which can be obtained from NCS measurements and give a number of examples of such measuremnts.

2.Theory of Measurements

The Impulse Approximation (IA) states that if the momentum lost by the incident neutron is sufficiently large, scattering occurs from a single atom with conservation of kinetic energy and momentum. Consider a scattering event in which a neutron loses momentum $\vec{q}$ and energy ω scattering from an atom of mass M. If the momentum of the atom is $\vec{p}$ before the collision, then from conservation of momentum it is $\vec{p}+\vec{q}$ after the collision and to conserve kinetic energy the equation

$$\omega = \frac{(\vec{p}+\vec{q})^2}{2M} - \frac{p^2}{2M} \qquad (1)$$

must be satisfied. Rearrangement of this equation gives

$$y = \vec{p}.\hat{\vec{q}} = \frac{M}{q}\left(\omega - \frac{q^2}{2M}\right) \qquad (2)$$

where $\hat{\vec{q}} = \vec{q}/|\vec{q}|$ is the unit vector along the direction of $\vec{q}$ and y is the component of atomic momentum along the direction of $\vec{q}$. In other words, from a measurement of the

neutron $\vec{q}$ and ω we can determine the component of the atomic momentum along the direction of $\vec{q}$. In the literature on neutron Compton scattering this component is generally denoted by the letter y as indicated in equation (2) and the linking of $\vec{q}$ and ω by equation 2 is known as 'y scaling' [20], a term which originated in deep inelastic studies of nucleon momentum components [21]. In an experiment we measure a large number of neutron-atom collisions and by recording the direction of $\hat{\vec{q}}$ and the value of y for each event we build up a distribution $J(\hat{\vec{q}}, y)$ (the 'directional Compton profile') which is proportional to the probability that an atom has momentum component y along the direction of $\hat{\vec{q}}$. One consequence of equation 2 is that if the neutron scatters from a stationary atom (y=0) the response lies along the 'recoil line' $\omega = q^2/(2M)$. In general $S(\vec{q},\omega)$ peaks at $\omega = q^2/(2M)$, but is broadened by the motion of the atoms in a similar way to the Doppler broadening of spectral lines by molecular motion. Thus the energy transferred from the neutron to the atom is mass dependent and this fact can be used to separate the contributions from different masses.

If the sample is an isotropic scatterer the direction of $\hat{\vec{q}}$ is immaterial and the 'directional Compton profile' $J(\hat{\vec{q}}, y)$ reduces to the 'Compton profile', $J(y)$- this is the probability that an atom has momentum component y along an arbitrary direction in space. The kinetic energy of atoms in isotropic samples is related to $J(y)$ via

$$\kappa = \frac{3}{2M}\int_{-\infty}^{\infty} y^2 J(y)dy \qquad (3)$$

The eVS spectrometer uses a filter difference method [22] to analyse the energy of the scattered neutrons. The filter is a thin foil of either gold or uranium, which absorbs neutrons strongly over narrow bands of energy. Two time of flight spectra are taken, one with the foil between the sample and detectors and the second with the foil removed. The difference between these spectra is due to neutrons absorbed in the foil and is effectively the time of flight spectrum for neutrons scattered with energy E_1. If E_1 is known, the momentum transfer $\vec{q}$ and energy transfer ω can be determined from a measurement of the neutron time of flight t in the usual way [23] and hence from equation 2, the atomic momentum component y can be found. In the inverse geometry configuration used on eVS the time of flight of the peak corresponding to a particular atomic mass decreases with atomic mass. Figure 1 shows time of flight spectra collected from a sample of amorphous

hydrogenated carbon [24] for a number of different scattering angles. The broad peak to the left of the spectra is due to scattering from hydrogen, while the smaller peak to the right is due to carbon scattering.

If it is a good approximation to treat the interaction of the atom studied with surrounding atoms as a single particle potential, NCS measurements have a particularly simple interpretation, From elementary quantum mechanics, $n(\vec{p})$ is related to the Fourier transform of the wavefunction $\Psi(\vec{r})$ via,

$$n(\vec{p}) = \frac{1}{(2\pi)^3}\left|\int \Psi(\vec{r})\exp(i\vec{p}.\vec{r})d\vec{r}\right|^2 \qquad (4)$$

and an NCS measurement of $n(\vec{p})$ can be used to determine the wavefunction in an analagous way to the determination of real space structure from a diffraction pattern.

3.Examples of Measurements

Measurements on liquid parahydrogen [25] gave very good agreement with the interpretation of $n(\vec{p})$ as the Fourier transform of the proton wave function. The wave function of the proton in the molecule is a spherical shell.

$$\Psi(r) = \left[2\pi^{3/2}\sigma(\sigma^2 + 2R^2)\right]^{-1/2}\exp\left[\frac{-(r-R)^2}{2\sigma^2}\right] \qquad (5)$$

where R is the bond length and the shell width σ is determined by the vibrational frequency. Figure 2 shows the deviation of the model and data from classical behaviour. The oscillations are the first observation of interference effects between the proton and neutron wavefunctions. This measurement also showed that the centre of mass molecular motion of diatomic molecules can be measured by NCS in different molecular environments, e.g. molecules in liquids or molecules in interstitial sites in solids. The peak shape of $J(y)$ contains important information about anisotropy and spatial distribution of the wavefunction even in isotropic samples such as liquids. In more complex molecular systems, further information can be obtained by measuring the momentum distributions of other atomic masses in the molecule. For example the centre of mass motion of water can be measured from a combination of the measurements on the hydrogen and oxygen atoms [26]

Measurements of atomic kinetic energies provide important information about the dynamics of any sample. Figure 3 shows the kinetic energy of Lithium measured between 20K and room temperature [27]. The line is the kinetic energy calculated from a phonon density of states determined from neutron scattering measurements of the phonon spectra . The measured kinetic energy was 10% higher than expected and this was attributed to anharmonicity of the lithium lattice vibrations. Measurements in the liquid phase are also planned.

One of the most important applications of NCS is to measurements of the kinetic energies of quantum fluids ^{3}He, ^{4}He, Ne and mixtures as a function of thermodynamic parameters such as temperature, concentration and pressure. eVS can provide momentum transfers and count rates which are orders of magnitudes greater than those available in NCS measurements on chopper spectrometers. Measurements on ^{3}He are particularly advantageous as the strong neutron absorption is much reduced at eV energies. Figure 4 shows a measurement of the kinetic energies of ^{3}He and ^{4}He atoms in mixtures of ^{3}He and ^{4}He as a function of concentration [28]. The results are very surprising and indicate that the ^{3}He kinetic energy is independent of composition, confirming an earlier measurement [29] made on the PHOENIX spectrometer at Argonne. Other recent measurements on quantum fluids have included measurements of the kinetic energies of Ne as a function of temperature [30] and ^{4}He as a function of temperature and pressure [31]. The former measurement allowed a comparison of our measurements with previous measurements on the chopper spectrometer HRMECS at ANL and with state of the art calculations. (Figure 5)

4. Future Developments

The future applications of NCS measurements from protons and deuterons are very wide. An example is the hydrogen bond where NCS can determine whether the observed bi-modal distribution of the proton in hydrogen bonds is the result of statistical or quantum disorder [32]. The information obtained from NCS is qualitatively different to that given by neutron diffraction measurements. The latter determine an infinite time average of the spatial distribution of the proton wheras the former measures the proton wavefunction on a very short timescale. Thus NCS can distinguish between quantum tunneling and thermally induced hopping of the proton between different sites. Detailed information

about the proton wavefunction can be obtained from single crystal samples, where NCS allows a model independent reconstruction of both the proton wavefunction and the potential well of the proton in three dimensions. Figure 6 shows a data collected from a single crystal of vanadium hydride [33]. There are clearly strong crystal symmetries present in the data and these can be directly related to form of the proton wavefunction.

As mentioned in section 2 the positions of peaks correponding to different atomic masses in time of flight spectra can be calculated. The amplitude of the peak from a particular mass M is determined by the sample composition and neutron scattering cross section, and the width of the peak depends upon the intrinsic width of $J(y)$ and instrument resolution function for mass M. In principle a fit can be made to the time of flight spectra with only a scale factor and the mean kinetic energies of different masses as fitting parameters. One routine future use of NCS will almost certainly be to determine the mean atomic kinetic energies of different masses in complicated samples as a function of thermodynamic parameters such as temperature, pressure and sample composition. Another application is to determine the bulk sample composition by including the peak amplitudes as fit parameters.

It should be emphasised that the NCS technique is still at a very early stage of development and that orders of magnitude increases in the accuracy of measurements can be expected as countrate and resolutions improve. The situation can be compared with electron Compton scattering where count rates have increased by five orders of magnitude during the last 30 years. Future NCS measurements will provide precise and unique information about the short time dynamics of many condensed matter systems of fundamental physical interest, again demonstrating the unique importance of neutrons as a probe of condensed matter.

References

1 P. C. Hohenberg and P. M. Platzmann, Phys Rev **152**, 198 (1966)

2 P. M. Platzmann in `Momentum Distributions', ed R. N. Silver and P. E. Sokol (Plenum Press,New York, 1989, p249)

3 I Sick in ref 2, page 175.

4 R Newton, 'Scattering Theory of Waves and Particles', (Springer, Berlin, 1981)

5 V. F. Sears Phys. Rev. B **30**, 44 (1984)

6 J. Mayers Phys. Rev. B **41**,41 (1991)

7 R. A. Cowley and A.D. B. Woods, Phys. Rev. Lett. **21**, 787 (1968)

8 O. K. Harling, Phys. Rev. Lett. **24,** 1046 (1970)

9 H. A. Mook, Phys. Rev. Lett. **32,** 1167 (1974)

10 H. A. Mook, Phys. Rev. Lett. **51**, 1454 (1983)

11 P. Martel, E. C. Svensson, A. D. B. Woods, V. F. Sears and R. A. Cowley, J. Low Temp. Phys. **23,** 285 (1976)

12 A. Griffin "Excitations in a Bose Condensed Liquid", (Cambridge University Press, 1993)

13 T. R. Sosnick, W. M. Snow, and P. E. Sokol, Phys. Rev. B **41**, 11185 (1990)

14 D. A. Peek, M. C. Schmidt, I. Fujita and R. O. Simmons, Phys. Rev. B **45**, 9671 (1992) and **45,** 9680 (1992)

15 H. Rauh and N. Watanabe, Phys. Lett. **100A**, 244 (1984)

16 M. P. Paoli and R. S. Holt, J. Phys. C **21**, 3633 (1988)

17 S. Ikeda, K. Shibata, Y. Nakai amd P. W. Stephens, J. Phys. Soc. Japan **61**, 2619 (1992)

18 J. Mayers and A. C. Evans, Rutherford Laboratory Report, RAL-91-048 (1991)

19 J Mayers "eVS User Guide", Internal RAL report (1994)

20 G. B. West in ref 2, p95.

21 G. B. West in ref 2, p95.

22 P. A. Seeger, A.D. Taylor and R.M. Brugger, Nuc Inst Meth **A240** 98 (1985)

23 C. G. Windsor, "Pulsed Neutron Scattering ", (Taylor and Francis, London, 1981)

24 J. Mayers, T.M. Burke and R.J. Newport, J. Phys. Condens. Matter **6** 641 (1994)

25 J Mayers, Phys Rev Lett **71** 1553 (1993).

26 C. Andreani, D. Colognesi and A. Filabozzi, unpublished.

27 A. C. Evans, J. Mayers and D. Timms, J. Phys Cond. Matter **6** 4197, (1994)

28 R. T. Azuah, W. G. Stirling, J. Mayers, I. F. Bailey and P. E. Sokol, submitted to J. Low Temp. Phys (1994)

29 Y. Wang and P.E. Sokol Phys Rev Lett **72** 1040 (1994)

30 D. N. Timms, A.C. Evans, M. Boninsegni, D. M. Ceperly, J. Mayers and R. O. Simmons, to be submitted to Phys Rev B.

31 C. Andreani, F. P. Ricci, J. Mayers, unpublished.

32 G. Reiter and R. N. Silver, Phys. Rev. Lett. **54**, 1047 (1985)

33 J. Etter, R Hempelmann, J Mayers, unpublished.

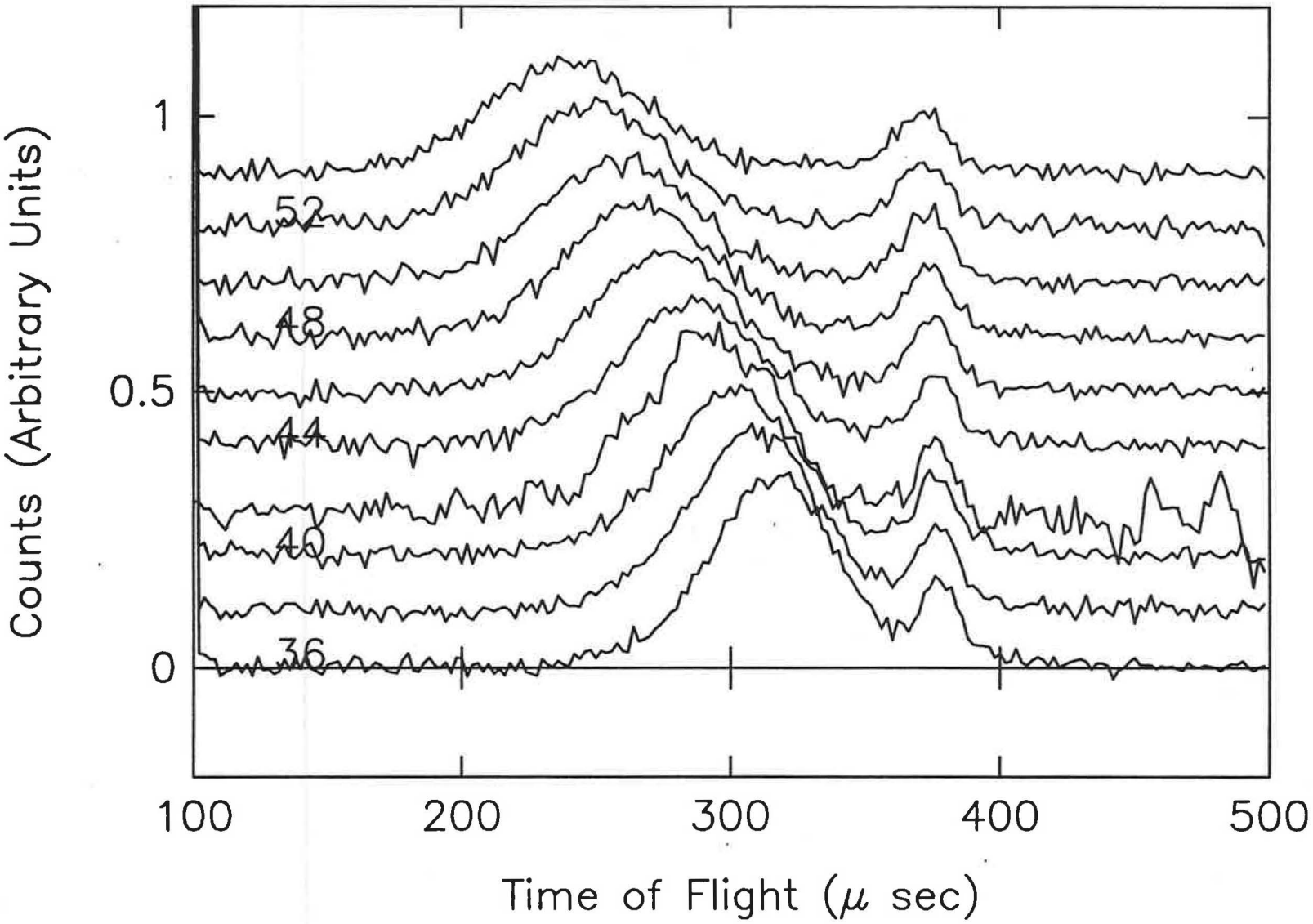

Figure1 Neutron time of flight spectra obtained from amorphous hydrogenated carbon (a-C:H) at ten different scattering angles from 36 to 54 . The separation of different atomic masses in time of flight can be seen. The left hand peak in each spectrum is due to scattering from hydrogen, the right hand peak is due to scattering from carbon. The peak separation increases with increasing scattering angle.

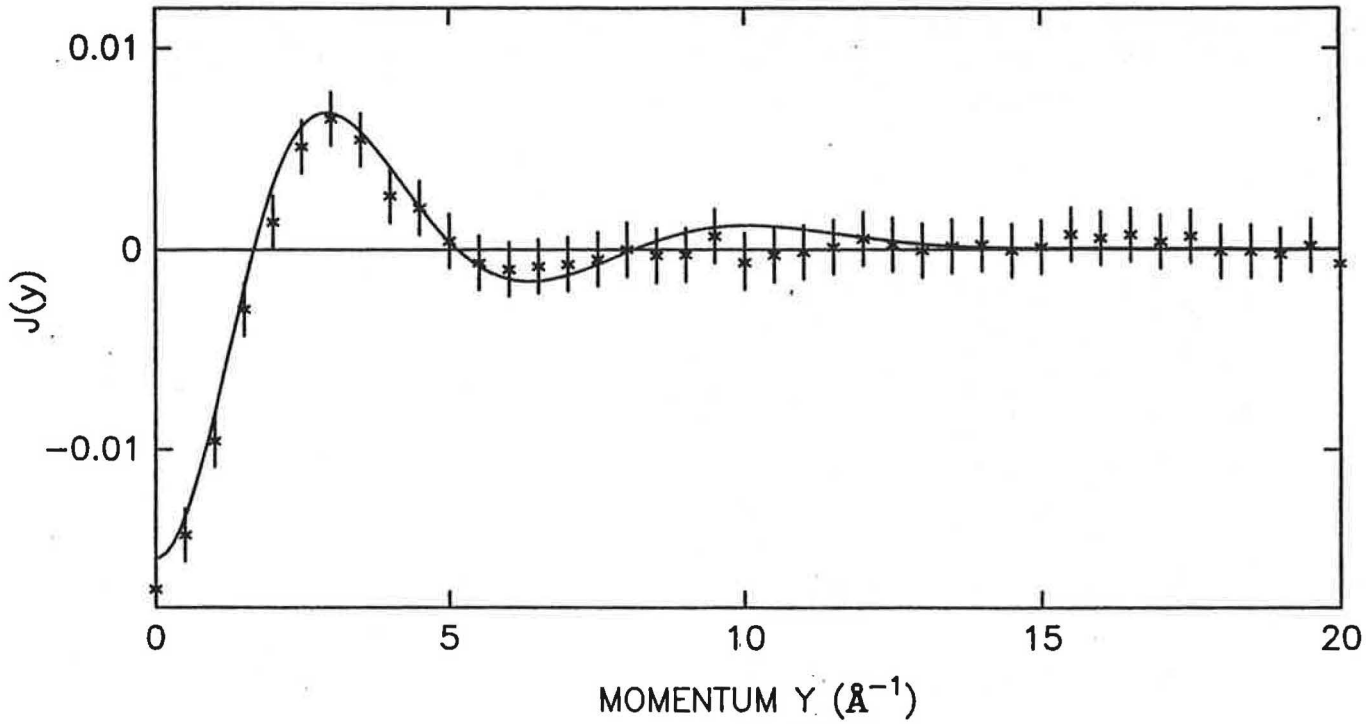

Figure 2 The solid line is the difference between classical and quantum models of the momentum distribution of the proton in molecular hydrogen. The points are the difference between the data and the classical model. The oscillations are due to the first observation of interference between the proton and neutron wavefunction.

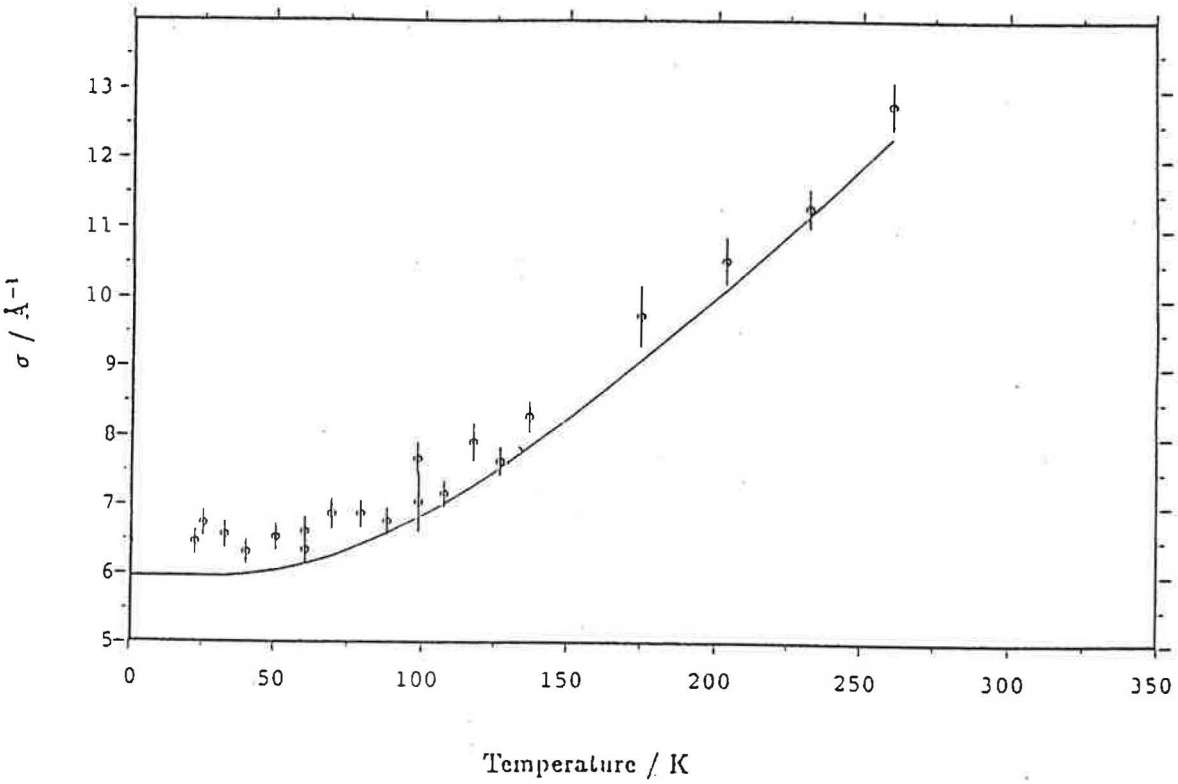

Figure 3 The points are measured values of the *r.m.s.* momentum of lithium atoms as a function of temperature. The line is a calculation assuming harmonic vibrations and using a phonon density of states calculated from a fit to neutron scattering data.

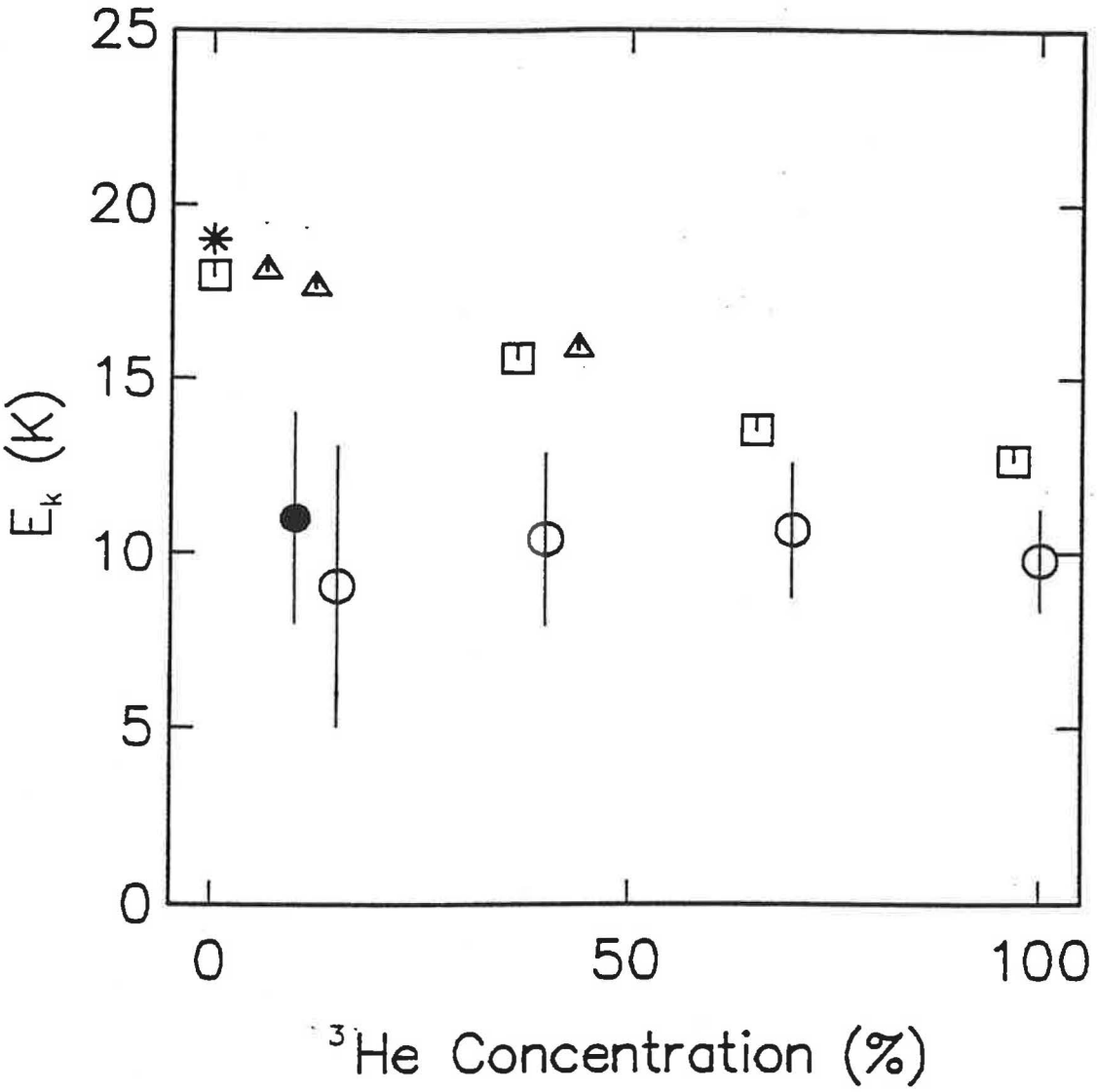

Figure 4 The kinetic energy of ^{3}He atoms in ^{3}He-^{4}He mixtures as a function of composition. The circles were measured on eVS while the solid circle is an earlier measurement performed on the PHOENIX spectrometer at A.N.L. The other points are theoretical calculations using various methods.

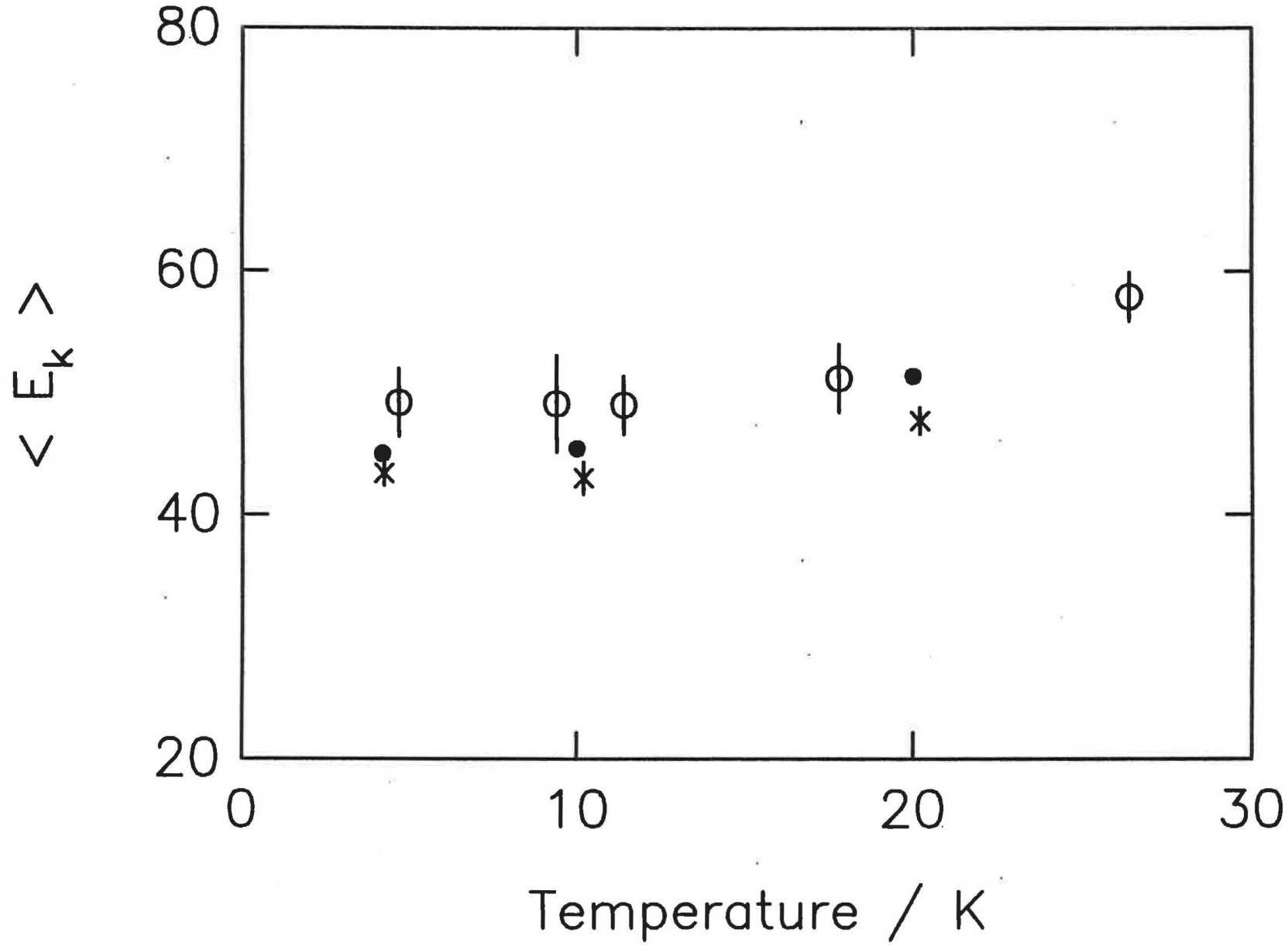

Figure 5 The kinetic energy of solid neon as a function of temperature. eVS data are shown as crosses, previous measurements as open circles. The solid circles are path integral Monte Carlo calculations.

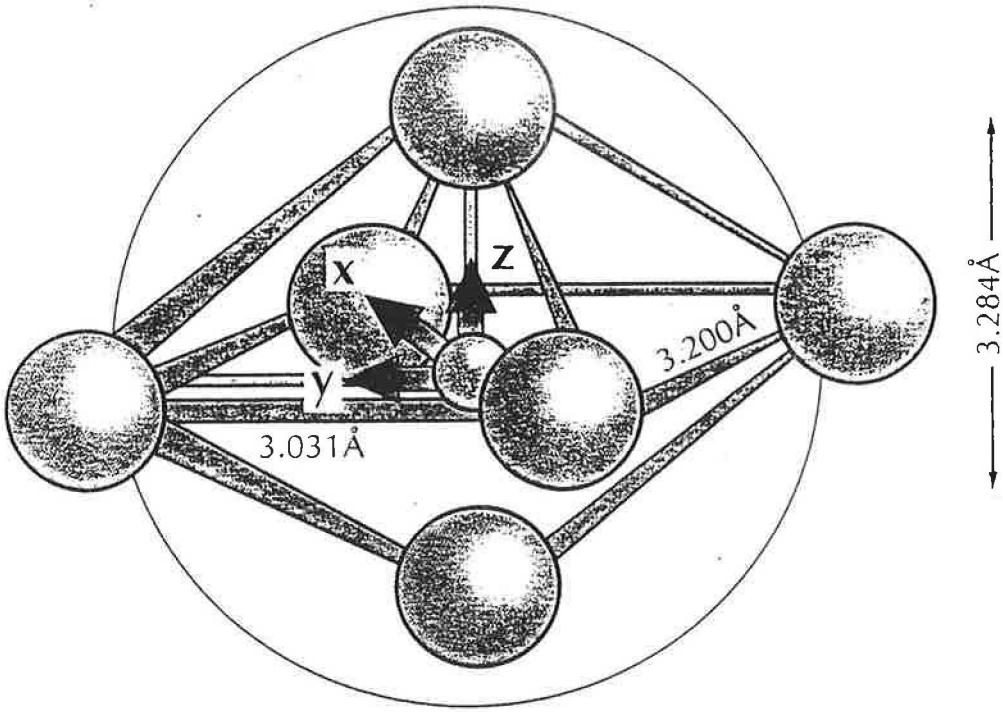

Figure 6 Measurement of the directional Compton profile $J(\vec{q}, y)$ for the proton in a single crystal of V_2H. The proton sits in an interstitial site surrounded by 6 vanadium atoms as shown in figure 6a. The measured Compton profile in the YZ plane is shown in figure 6b. The strong crystal symmetries observable in the raw data are due to Fourier components of the proton wavefunction.